Eur. Phys. J. D **2**, 237–243 (1998)

THE EUROPEAN PHYSICAL JOURNAL D

Dressing modification in the laser-assisted proton-helium charge exchange collision

S.-M. Li[1,2,a], X.-L. Xu[3], Z.-F. Zhou[2], J. Chen[1,2], and Y.-Y. Liu[2]

[1] Chinese Center of Advanced Science and Technology (World Laboratory), P.O. Box 8730, Beijing 100080, P.R. China
[2] Department of Modern Physics, University of Science and Technology of China, P.O. Box 4, Hefei, Anhui 230027, P.R. China
[3] Department of Physics, University of Hong Kong, Pokfulam Road, Hong Kong

Received: 9 April 1997 / Revised: 24 September 1997 / Received in final form: 25 November 1997 / Accepted: 5 February 1998

Abstract. A first Born approach to intense laser modified proton-helium electron capture collision is given. Theoretical results show that the angular distribution peaks forward sharply. For a geometry of laser polarization vector parallel to the incident direction, the dressing effect on the differential cross section covers a relatively wide angular range; while for a perpendicular geometry, the result is modified only in a very small angular region. The integral cross sections get highly promoted by laser with the impact energy increasing. The modified cross sections are increasing functions of field strength, but decreasing functions of field frequency. Comparisons with the laser assisted electron capture from atomic hydrogen are made.

PACS. 34.50.Rk Laser-modified scattering and reactions – 34.70.+e Charge transfer – 32.80.Wr Other multiphoton processes

1 Introduction

A recent paper of this series [1] has dealt with the intense laser assisted electron capture into the dressed ground state of hydrogen in the collision of a proton with a dressed hydrogen atom. The results showed that the presence of a laser background promotes the capture cross sections significantly.

For target atoms which possess more than one electron, an investigation into the dressing effect on charge transfer cross sections is necessary. Experimental test of such captures may be more feasible than the capture from atomic hydrogen. In this paper, we calculate the simplest case,

$$p + \mathrm{He} \xrightarrow{Laser} \mathrm{H} + \mathrm{He}^{+}. \tag{1.1}$$

As in the preceding work, the laser field is treated as a linearly polarized classical electromagnetic field,

$$\mathbf{A} = \mathbf{A}_0 \cos\omega t = \frac{c}{\omega}\boldsymbol{\varepsilon}_0 \cos\omega t \tag{1.2}$$

where $\boldsymbol{\varepsilon}_0$ is the electric vector of the field. The field strength is supposed to be far less than one atomic unit (*i.e.* the Coulomb field strength at the first Bohr radius of the hydrogen atom).

In the laser-free case, electron capture has been extensively studied during the past decades [2,3]. For capture from hydrogen and helium targets, the first Born approximation (FBA) seems to agree with experiment well, at least in the intermediate and high energy range [4–7]. With this in mind, the FBA is employed in the present calculation to treat the proton-dressed-helium scattering.

The arrangement of this paper is as follows. In Section 2, we extend the theoretical treatment in reference [1] to treat the laser-assisted electron capture from helium. In Section 3, the laser modified cross sections and their dependence on each laser parameter are discussed. Section 4 is concluding remarks. Some comparisons with the capture from a hydrogen target are made. The atomic units $e = m = 1$ are used throughout in all computations, although in some figures the common units are used for explicitness.

2 Theory

For reaction (1.1), we choose the coordinate system as shown in Figure 1. Let the origin be on the target nucleus (N). The masses are labeled as follows: M_P = proton, M_N = helium nucleus, $m = 1$ = electron. The laboratory particle coordinates are defined as $\mathbf{r}_0$ = proton, $\mathbf{r}_{1,2}$ = electrons. Then the relative coordinates of initial and final states are,

$$\mathbf{R} = \mathbf{r}_0 - (\mathbf{r}_1 + \mathbf{r}_2)/(M_N + 2) \tag{2.1}$$

$$\mathbf{R}' = (M_P\mathbf{r}_0 + \mathbf{r}_1)/(M_P + 1) - \mathbf{r}_2/(M_N + 1). \tag{2.2}$$

[a] e-mail: lism@lx04.mphy.ustc.edu.cn

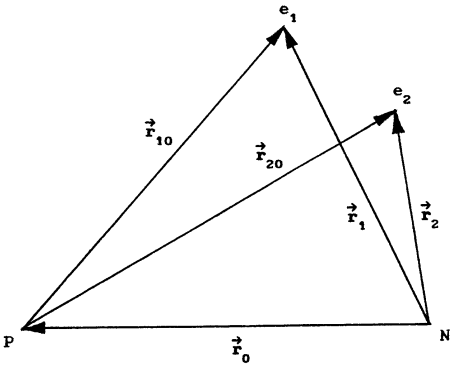

Fig. 1. The coordinate system used for description of the laser-assisted proton-helium electron capture collision.

In FBA, the S-matrix element for the electron capture of proton from a dressed ground state helium into a dressed ground state hydrogen is,

$$S^{B_1} = -i\sqrt{2}\int_{-\infty}^{\infty} dt < \chi_F(\mathbf{R}',t)\psi_0^{\mathrm{H}}(\mathbf{r}_{10},t)\psi_0^{\mathrm{He}^+}(\mathbf{r}_2,t)| V_{I,F}|\chi_I(\mathbf{R},t)\psi_0^{\mathrm{He}}(\mathbf{r}_1,\mathbf{r}_2,t) > \quad (2.3)$$

where χ_I and χ_F represent, respectively, the incoming plane wave of proton and the outgoing plane wave of the newly formed atomic hydrogen in final state. ψ_0^{H}, $\psi_0^{\mathrm{He}^+}$, and ψ_0^{He} denote the laser dressed wave functions of the final state hydrogen, the residual helium ion, and the target helium respectively. $V_{I,F}$ is the prior or post interaction. It is well-established that the prior and post cross sections are equal provided that the exact atomic wave functions are used in the S-matrix element [5]. Since only the approximate atomic wave functions are available in the present calculation, some discrepancy may occur. However, for the laser-free case, the discrepancy is quite small [7], and we would expect the discrepancy to be also small in the laser modified case. It is more practical to use the prior form of interaction which presents less complexity in calculations.

For a ground state atom A, the dressed wavefunction in soft-photon approximation is given by [8],

$$\psi_0^A(\mathbf{x}_1,\cdots,\mathbf{x}_A,t) = e^{-iW_0^A t}\left[\phi_0^A(\mathbf{x}_1,\cdots,\mathbf{x}_A) - \cos\omega t\ \widetilde{\phi}_0^A(\mathbf{x}_1,\cdots,\mathbf{x}_A)\right] \quad (2.4)$$

where

$$\widetilde{\phi}_0^A(\mathbf{x}_1,\cdots,\mathbf{x}_A) = \frac{1}{\omega_A c}\mathbf{A}_0\cdot\sum_{j=1}^{A}\mathbf{p}_j\phi_0^A(\mathbf{r}_1,\cdots,\mathbf{x}_A) = -\frac{i}{\omega_A\omega}\boldsymbol{\varepsilon}_0\cdot\sum_{j=1}^{A}\nabla_{\mathbf{x}_j}\phi_0^A(\mathbf{r}_1,\cdots,\mathbf{x}_A) \quad (2.5)$$

ϕ_0^A is the ground state wave vector for the laser-free case, the binding energy of which is W_0^A, and ω_A is the average excitation energy [9].

Substituting the wavefunctions for each dressed atom and ion into equation (2.3), and working out the time integration, we obtain the S-matrix element in the form

$$S^{B_1} = \frac{i}{2\pi}\sum_{l=-1}^{+1} f_l^{B_1}\delta(E_F + W_0^{\mathrm{H}} + W_0^{\mathrm{He}^+} - E_I - W_0^{\mathrm{He}} + l\omega) \quad (2.6)$$

in which

$$f_0^{B_1} = f^{B_1}(\phi_0^{\mathrm{He}} \longrightarrow \phi_0^{\mathrm{H}}\phi_0^{\mathrm{He}^+}) \quad (2.7)$$

$$f_{\pm1}^{B_1} = f^{B_1}(\widetilde{\phi}_0^{\mathrm{He}} \longrightarrow \phi_0^{\mathrm{H}}\phi_0^{\mathrm{He}^+}) + f^{B_1}(\phi_0^{\mathrm{He}} \longrightarrow \widetilde{\phi}_0^{\mathrm{H}}\phi_0^{\mathrm{He}^+}) + f^{B_1}(\phi_0^{\mathrm{He}} \longrightarrow \phi_0^{\mathrm{H}}\widetilde{\phi}_0^{\mathrm{He}^+}) \quad (2.8)$$

are scattering amplitudes corresponding to the transfer of $l = 0$, and ±1 photons between the collision system and the laser field. Here we have dropped the transitions between dressed terms. The scattering amplitude of equation (2.7) for the laser-free case can be written as

$$\begin{aligned} f_0^{B_1} &= -\frac{\mu_F}{2\pi}\int d^3(Rr_1r_2)e^{-i\mathbf{k}_F\cdot\mathbf{R}'}e^{i\mathbf{k}_I\cdot\mathbf{R}} \times \phi_0^{\mathrm{H}*}(\mathbf{r}_{10})\phi_0^{\mathrm{He}^+*}(\mathbf{r}_2)V_I\phi_0^{\mathrm{He}}(\mathbf{r}_1,\mathbf{r}_2) \\ &= -\frac{\mu_F}{2\pi}\int d^3(r_0r_1r_2)e^{-i\mathbf{q}_0\cdot\mathbf{r}_0}e^{-i\mathbf{q}_1\cdot\mathbf{r}_1}e^{-i\mathbf{q}_2\cdot\mathbf{r}_2} \times \phi_0^{\mathrm{H}*}(\mathbf{r}_{10})\phi_0^{\mathrm{He}^+*}(\mathbf{r}_2)V_I\phi_0^{\mathrm{He}}(\mathbf{r}_1,\mathbf{r}_2) \end{aligned} \quad (2.9)$$

where $\mu_F = (M_P+1)(M_N+1)/(M_P+M_N+2)$ is the reduced mass of the final state. $\mathbf{q}_0$, $\mathbf{q}_1$ and $\mathbf{q}_2$ are the momenta transfer of the proton, the transferred electron e_1, and the passive electron e_2 respectively,

$$\mathbf{q}_0 = \mathbf{k}_F M_P/(M_P+1) - \mathbf{k}_I \quad (2.10)$$

$$\mathbf{q}_1 = \mathbf{k}_F/(M_P+1) + \mathbf{k}_I/(M_N+2) \quad (2.11)$$

$$\mathbf{q}_2 = -\mathbf{k}_F/(M_N+1) + \mathbf{k}_I/(M_N+2). \quad (2.12)$$

Because the momentum transfer of the passive electron is much less than that of the incident proton and of the captured electron, we may set $q_2 \approx 0$ to simplify the calculation [6]. Equation (2.9) is then reduced to

$$f_0^{B_1} = -\frac{\mu_F}{2\pi}\int d^3(r_0r_1r_2)e^{-i\mathbf{q}_0\cdot\mathbf{r}_0}e^{-i\mathbf{q}_1\cdot\mathbf{r}_1} \times \phi_0^{\mathrm{H}*}(\mathbf{r}_{10})\phi_0^{\mathrm{He}^+*}(\mathbf{r}_2)\left(\frac{2}{r_0} - \frac{1}{r_{10}} - \frac{1}{r_{20}}\right)\phi_0^{\mathrm{He}}(\mathbf{r}_1,\mathbf{r}_2). \quad (2.13)$$

We chose the approximate ground state wave function of helium in the Hartree-Fock form [10],

$$\phi_0^{\mathrm{He}}(\mathbf{r}_1,\mathbf{r}_2) = \phi_0(\mathbf{r}_1)\phi_0(\mathbf{r}_2) \quad (2.14)$$

where

$$\phi_0(\mathbf{r}) = \frac{1}{\sqrt{4\pi}} \sum_{i=1}^{2} C_i e^{-\alpha_i r} \tag{2.15}$$

with $C_1 = 2.60505$, $C_2 = 2.08144$, $\alpha_1 = 1.41$, and $\alpha_2 = 2.61$. Then the amplitude equation (2.13) can be reduced to parametric differentiations of a numerical integral. That is

$$f_0^{B_1} = 16\mu_F \sum_{i,j=1}^{2} C_i C_j I_{ij} \tag{2.16}$$

in which

$$\begin{aligned} I_{ij} = {} & \frac{2}{\beta_j^3}\frac{\partial}{\partial\alpha_i}\left(\frac{\partial}{\partial\lambda} - \frac{\partial}{\partial\gamma}\right) I(\mathbf{q}_0, \gamma, \mathbf{q}_1, \alpha_i, \lambda) \\ & + \left(\frac{2}{\beta_j^3} - \frac{1}{\beta_j^2}\frac{\partial}{\partial\beta_j}\right)\frac{\partial^2}{\partial\alpha_i\partial\lambda} I(\mathbf{q}_0, \beta_j, \mathbf{q}_1, \alpha_i, \lambda) \end{aligned} \tag{2.17}$$

where [8],

$$I(\mathbf{q}_0, \beta, \mathbf{q}_1, \alpha, \lambda) = \int_0^1 d\xi \frac{1}{\rho[(\rho+\beta)^2 + q^2]} \tag{2.18}$$

with

$$\mathbf{q} = \mathbf{q}_0 + \mathbf{q}_1\xi \tag{2.19}$$

$$\rho = [\lambda^2 + (q_1^2 + \alpha^2 - \lambda^2)\xi - q_1^2\xi^2]^{1/2}. \tag{2.20}$$

In computing equation (2.17), we set $\gamma = 0$, $\lambda = 1$, and $\beta_j = \alpha_j + 2$ $(j = 1, 2)$. In the same way, we obtain the dressed parts of the scattering amplitude,

$$\begin{aligned} f_{\pm1}^{B_1} = {} & -\frac{\mu_F}{2\pi}\int d^3(Rr_1r_2) e^{-i\mathbf{k}_F\cdot\mathbf{R}'} e^{i\mathbf{k}_I\cdot\mathbf{R}} \\ & \times \Big[\widetilde{\phi}_0^{\mathrm{H}*}(\mathbf{r}_{10})\phi_0^{\mathrm{He}^+*}(\mathbf{r}_2) V_I \phi_0^{\mathrm{He}}(\mathbf{r}_1, \mathbf{r}_2) \\ & + \phi_0^{\mathrm{H}*}(\mathbf{r}_{10})\widetilde{\phi}_0^{\mathrm{He}^+*}(\mathbf{r}_2) V_I \phi_0^{\mathrm{He}}(\mathbf{r}_1, \mathbf{r}_2) \\ & + \phi_0^{\mathrm{H}*}(\mathbf{r}_{10})\phi_0^{\mathrm{He}^+*}(\mathbf{r}_2) V_I \widetilde{\phi}_0^{\mathrm{He}}(\mathbf{r}_1, \mathbf{r}_2)\Big] \\ \approx {} & -\frac{\mu_F}{2\pi}\int d^3(r_0r_1r_2) e^{-i\mathbf{q}_0\cdot\mathbf{r}_0} e^{-i\mathbf{q}_1\cdot\mathbf{r}_1} \\ & \times \Big[\widetilde{\phi}_0^{\mathrm{H}*}(\mathbf{r}_{10})\phi_0^{\mathrm{He}^+*}(\mathbf{r}_2) V_I \phi_0^{\mathrm{He}}(\mathbf{r}_1, \mathbf{r}_2) \\ & + \phi_0^{\mathrm{H}*}(\mathbf{r}_{10})\widetilde{\phi}_0^{\mathrm{He}^+*}(\mathbf{r}_2) V_I \phi_0^{\mathrm{He}}(\mathbf{r}_1, \mathbf{r}_2) \\ & + \phi_0^{\mathrm{H}*}(\mathbf{r}_{10})\phi_0^{\mathrm{He}^+*}(\mathbf{r}_2) V_I \widetilde{\phi}_0^{\mathrm{He}}(\mathbf{r}_1, \mathbf{r}_2)\Big]. \end{aligned} \tag{2.21}$$

Using the exponential-parameter integration technique developed earlier [11], it is easy to obtain the dressed amplitudes in the form

$$f_{\pm1}^{B_1} = 16\mu_F \sum_{i,j=1}^{2} C_i C_j \widetilde{I}_{ij} \tag{2.22}$$

where

$$\begin{aligned} \widetilde{I}_{ij} = {} & \frac{2}{\beta_j^3}\Big[-u\frac{\partial^2}{\partial\alpha_i\partial q_{0\varepsilon}} + \left[u\frac{\partial}{\partial\alpha_i} + v_i\left(\frac{\partial}{\partial\lambda} - \frac{\partial}{\partial\gamma}\right)\right] \\ & \times \frac{\partial}{\partial q_{1\varepsilon}} I(\mathbf{q}_0, \gamma, \mathbf{q}_1, \alpha_i, \lambda)\Big] \\ & + \left(\frac{2}{\beta_j^3} - \frac{1}{\beta_j^2}\frac{\partial}{\partial\beta_j}\right)\Big[-u\frac{\partial^2}{\partial\alpha_i\partial q_{0\varepsilon}} \\ & + \left(u\frac{\partial}{\partial\alpha_i} + v_i\frac{\partial}{\partial\lambda}\right)\frac{\partial}{\partial q_{1\varepsilon}} I(\mathbf{q}_0, \beta_j, \mathbf{q}_1, \alpha_i, \lambda)\Big] \\ & + w_j\frac{2}{\beta_j^4}\frac{\partial^2}{\partial\alpha_i\partial\lambda} J(\mathbf{q}_0, \gamma, \mathbf{q}_1, \alpha_i, \lambda) \\ & - w_j\left(\frac{2}{\beta_j^4} - \frac{2}{\beta_j^3}\frac{\partial}{\partial\beta_j} + \frac{1}{\beta_j^2}\frac{\partial}{\partial\beta_j^2}\right) \\ & \times \frac{\partial^2}{\partial\alpha_i\partial\lambda} J(\mathbf{q}_0, \beta_j, \mathbf{q}_1, \alpha_i, \lambda) \\ & - u\frac{2}{\beta_j^3} T(\mathbf{q}_0, \lambda, \mathbf{q}_1 + \mathbf{q}_0, \alpha_i). \end{aligned} \tag{2.23}$$

In the equation above, $u = -\lambda\varepsilon_0/(\omega\omega_{\mathrm{H}})$, $v_i = -\alpha_i\varepsilon_0/(\omega\omega_{\mathrm{He}})$, $w_j = (\varepsilon_0/\omega)(\alpha_j/\omega_{\mathrm{He}} - 2/\omega_{\mathrm{He}^+})$. The basic integrals J and T are given by

$$J(\mathbf{q}_0, \beta, \mathbf{q}_1, \alpha, \lambda) = \int_0^1 d\xi \frac{q_\varepsilon}{q^3}\frac{\rho+\beta}{\rho}\left(\frac{\pi}{2} - \arctan\frac{\rho+\beta}{q}\right) \tag{2.24}$$

$$T(\mathbf{q}_0, \beta, \mathbf{q}_1, \alpha) = \frac{4\alpha}{(\alpha^2 + q_1^2)^2}\frac{q_{0\varepsilon}}{q_0^3}\left(\frac{\beta q_0}{\beta^2 + q_0^2} - \arctan\frac{q_0}{\beta}\right) \tag{2.25}$$

where q and ρ are defined by equations (2.19) and (2.20), respectively.

According to the S-matrix of equation (2.6), the dressed charge transfer cross section is a sum over all partial cross sections which correspond to a certain number of photons exchanged,

$$\begin{aligned} \frac{d\sigma^{B_1}}{d\Omega} &= \sum_{l=-1}^{+1} \frac{d\sigma_l^{B_1}}{d\Omega} \\ &= \sum_{l=-1}^{+1} \frac{k_F}{k_I} |f_l^{B_1}|^2. \end{aligned} \tag{2.26}$$

3 Results and discussion

In Figure 2 we give the differential cross sections for electron capture of a proton from a dressed ground state helium into a dressed ground state hydrogen in the center of mass system. The impact energy is $E_L = 1000$ keV (measured in laboratory system). The field strength is

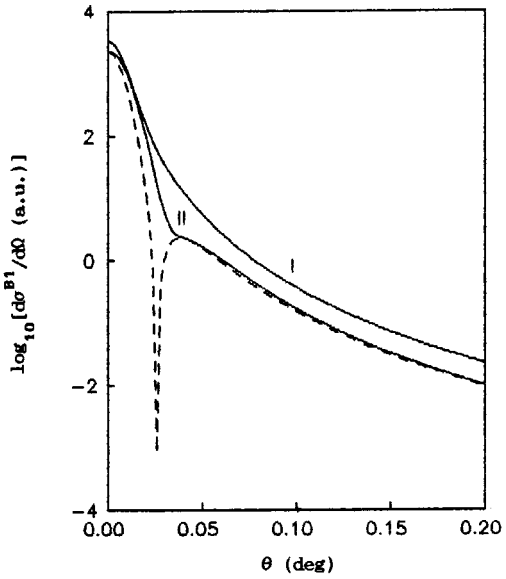

Fig. 2. The laser-modified differential cross section for electron capture from a dressed ground state helium into the dressed ground state of the final hydrogen in the center of mass system. The impact energy is $E_L = 1000$ keV (measured in laboratory system), field strength $\varepsilon_0 = 10^8$ V cm^{-1}, photon energy $\hbar\omega = 1.0$ eV. Solid curve I: dressed cross section for a parallel geometry $\boldsymbol{\varepsilon}_0 \parallel \mathbf{k}_I$. Solid curve II: dressed cross section for a perpendicular geometry $\boldsymbol{\varepsilon}_0 \perp \mathbf{k}_I$. Dashed curve: cross section for the laser-free case.

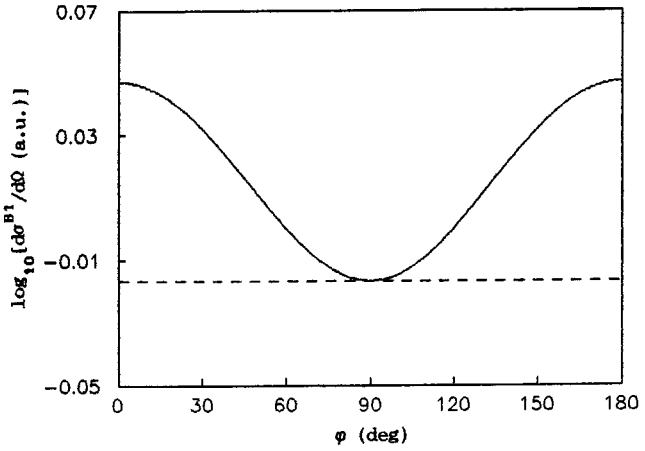

Fig. 3. The differential cross section in a perpendicular geometry as a function of azimuth angle at $\theta = 0.06°$, with $E_L = 1000$ keV, $\varepsilon_0 = 10^8$ V cm^{-1}, $\hbar\omega = 1.0$ eV. Solid curve: dressed cross section. Dashed curve: cross section for the laser-free case.

$\varepsilon_0 = 1.0\times10^8$ V cm^{-1}, frequency $\hbar\omega = 1.0$ eV. Solid curves I and II represent the laser-modified cross section for geometries $\boldsymbol{\varepsilon}_0 \parallel \mathbf{k}_I$ and $\boldsymbol{\varepsilon}_0 \perp \mathbf{k}_I$ respectively. The dashed curve is the result for the laser-free case. It is known there is a non-physical dip in the field-free cross section, however this dip does not appear in the laser-modified cross sections. As a matter of fact, the dip that appears in the

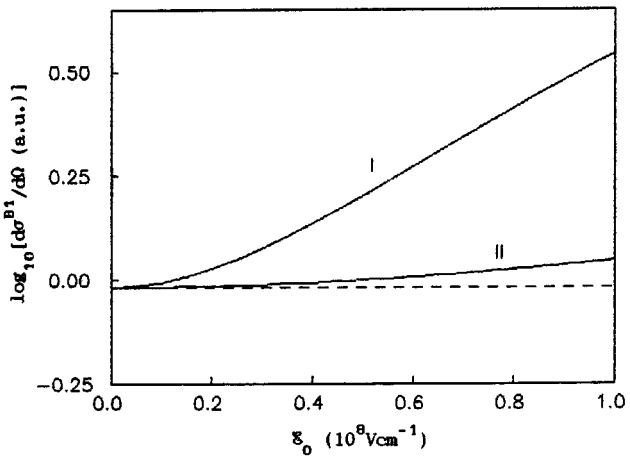

Fig. 4. The relation between differential cross sections and field strength at fixed frequency $\hbar\omega = 1.0$ eV, with $E_L = 1000$ keV, $\theta = 0.06°$. Solid curve I: laser-modified cross section for $\boldsymbol{\varepsilon}_0 \parallel \mathbf{k}_I$. Solid curve II: laser-modified cross section for $\boldsymbol{\varepsilon}_0 \perp \mathbf{k}_I$. Dashed curve: result for the laser-free case.

FBA cross section is caused by the strong cancellation between the scattering potentials [12], but does not appear in other calculations [13,14]. The same feature also occurs in each partial cross section of equation (2.26) (the curves for partial cross sections $d\sigma_l^{B_1}/d\Omega$ are not presented in the figure). Because the dip positions of each partial cross section are slightly different, thereby in the sum cross section $\sum_{l=-1}^{+1} d\sigma_l^{B_1}/d\Omega$ the dips are smoothed out. Both the dressed results for a parallel geometry and for a perpendicular geometry have no dips. For a parallel geometry, the modified cross section is greater than that for laser absence throughout the angular range we considered. While for a perpendicular geometry, the cross section is more sharply focused forwardly just like that for laser absence. At $\theta \sim 0°$, the result for a perpendicular geometry is a little higher than that for a parallel one. With angle increasing, the former is gradually surpassed by the latter. When the scattering angle exceeds 0.04°, the laser modification for a parallel geometry nearly disappears.

When the polarization vector of laser is not in the incident direction of proton, the collision is generally asymmetric about the z-axis, and the differential cross sections become azimuth-angle-dependent. Figure 3 describes the cross section as a function of azimuth angle for geometry $\boldsymbol{\varepsilon}_0 \perp \mathbf{k}_I$, at a scattering angle $\theta = 0.06°$ ($\boldsymbol{\varepsilon}_0$ is set in the xz plane). At $\varphi = 0°$, the curve gains its maximum, then drops to a minimum at $\varphi = 90°$ (the minimum is nearly the same as the corresponding cross section for laser-free). Because of the symmetric geometry, the curve is symmetric about $\varphi = 90°$.

In Figures 4-6, we exhibit the differential cross section dependence on laser strength, frequency and polarization direction. We find that the cross sections are increasing functions of field strength, but decreasing factions of laser frequency. This is consistent with equation (2.5).

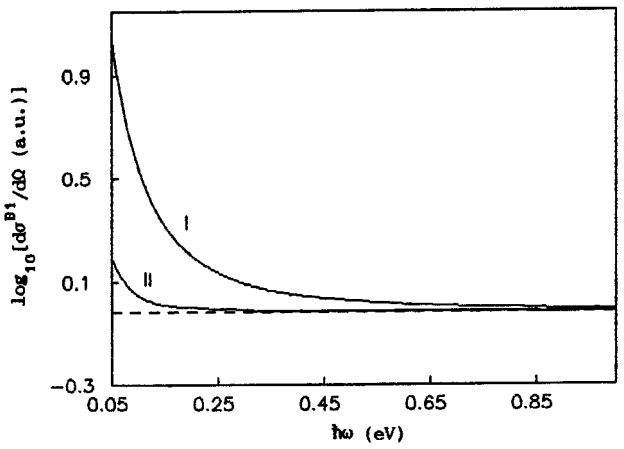

Fig. 5. The relation between differential cross sections and laser frequency at fixed field strength $\varepsilon_0 = 10^7\,\mathrm{V\,cm^{-1}}$, and $E_L = 1000$ keV, $\theta = 0.06°$. Solid curve I: dressed result for $\boldsymbol{\varepsilon}_0 \parallel \mathbf{k}_I$. Solid curve II: dressed result for $\boldsymbol{\varepsilon}_0 \perp \mathbf{k}_I$. Dashed curve: result for the laser-free case.

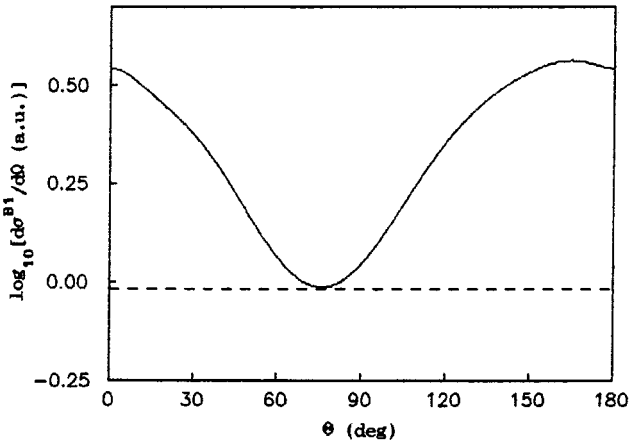

Fig. 6. Differential cross section dependence on polarization direction at $\theta = 0.06°$, $\varphi = 0°$, with $E_L = 1000$ kev, $\varepsilon_0 = 10^8$ V cm^{-1}, $\hbar\omega = 1.0$ eV. Solid line: laser present. Dashed line: laser free.

Especially for $\boldsymbol{\varepsilon}_0 \parallel \mathbf{k}_I$, the dressing effect is notable. Figure 6 shows that the dressed cross section is a periodic function of the polarization direction. This is quite different from the corresponding result for the laser-assisted proton-hydrogen electron capture. The difference is essentially caused by the different electron cloud distributions between the dressed hydrogen and helium targets.

Figure 7 displays the integral capture cross sections in the energy range where the laser-free cross section agrees well with experiment. The black dots denote the experimental result of Barnett *et al.* for a laser-free case [4, 15], in which the capture into all hydrogen states are included. Since in the present calculation only capture into the ground state is considered, the agreement for the laser-free case is better than the dashed curve would indicate. Figure 7 shows that the laser assisted total capture cross

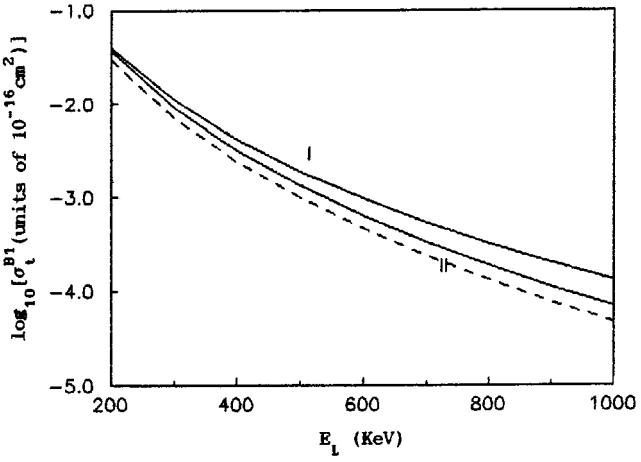

Fig. 7. Integral cross section for laser-assisted ground state electron capture at $\varepsilon_0 = 10^8\,\mathrm{V\,cm^{-1}}$, $\hbar\omega = 1.0$ eV. Solid curve I: result for $\boldsymbol{\varepsilon}_0 \parallel \mathbf{k}_I$. Solid curve II: result for $\boldsymbol{\varepsilon}_0 \perp \mathbf{k}_I$. Dashed curve: result for laser-free case. Black dots: experimental result of Barnett *et al.* for capture into all hydrogen states in laser absence.

section is larger than the field-free cross section, and this difference steadily increase with the impact energy. This seems in contradiction with the conclusion of Byron *et al.* [9] and our earlier calculation on $e^+ - \mathrm{H}$ rearrangement collision [8]. In fact at high energy, unlike other collisions in which the nucleus-nucleus interaction gives the dominant contribution (the internuclear interaction is not affected by the electron state of the target), the electron capture collision is dominated by the nucleus-electron interaction, and the internuclear potential gives no contribution [3,16, 17]. Therefore the capture cross section is quite sensitive to the electron states of the target in a certain energy range. Even for $e^+ - \mathrm{H}$ rearrangement collision, the difference between the dressed total capture cross section and the laser-free cross section also increases with E_L at higher energy [18]. The curves also show that a parallel geometry leads to greater cross sections than a perpendicular geometry does.

Figures 8 and 9 demonstrate the dependence of the integral cross sections with respect to the field strength and photon energy. In both geometries, the laser-modified cross sections go up with the field intensity, but drop down with frequency. With $\varepsilon_0 \to 0$ or $\omega \to \infty$, the cross sections approach the asymptotic value, the laser-free result. Figure 10 depicts the dependence of the integral cross sections on polarization direction. The dressing effect reaches its highest when the electric vector is parallel or antiparallel to the incident direction; and is at its lowest when the electric vector is perpendicular to it.

4 Concluding remarks

We have applied the laser-assisted collision theory to the electron capture in collisions between protons and helium targets. From the results obtained, we find that the laser

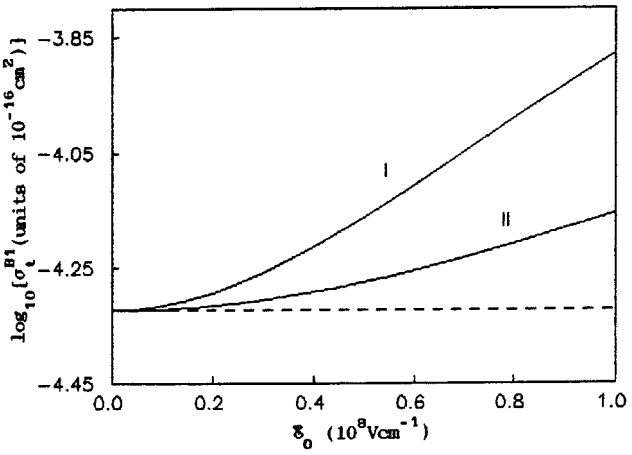

Fig. 8. Dressed integral cross sections as functions of field strength at $\hbar\omega = 1.0$ eV, $E_L = 1000$ keV. Solid curve I: result for $\boldsymbol{\varepsilon}_0 \parallel \mathbf{k}_I$. Solid curve II: result for $\boldsymbol{\varepsilon}_0 \perp \mathbf{k}_I$. Dashed line: result for laser-free.

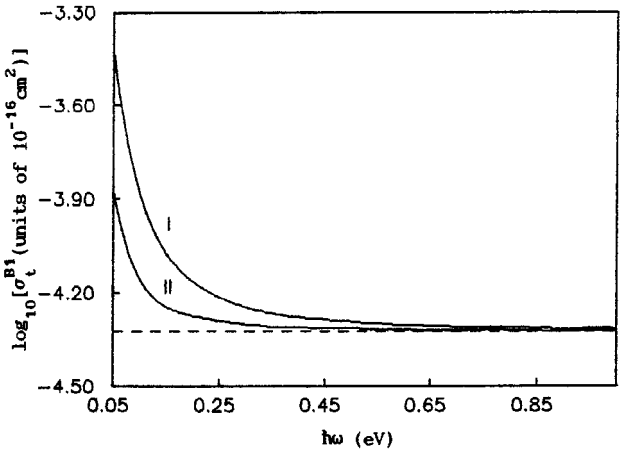

Fig. 9. Laser-modified integral cross sections against field frequency at fixed strength $\varepsilon_0 = 10^7\,\mathrm{V\,cm^{-1}}$, with $E_L = 1000$ keV. Solid curve I: result for $\boldsymbol{\varepsilon}_0 \parallel \mathbf{k}_I$. Solid curve II: result for $\boldsymbol{\varepsilon}_0 \perp \mathbf{k}_I$. Dashed curve: result for laser-free case.

modified cross sections for capture from hydrogen and from helium have some common features: for instance, the laser field promotes the capture cross sections, and the cross sections are increasing functions of laser strength, and decreasing functions of laser frequency. However we observe some significant differences in these two cases.

For capture from hydrogen targets, the laser modification on differential cross sections for both parallel and perpendicular geometries disappears at large scattering angle. However, for the helium targets, the laser promotion for a parallel geometry covers quite a wide angular range. This implies that even when the proton "penetrates" into the target helium, the passive-electron-proton interaction contributes to capture cross sections. If the passive electron happens to be on the side opposite to the transferred electron, its attraction on proton will reduce the repulsion of the target nucleus. According to the mechanism we suggest, the field can only change the cross section through the dressed electron. Thus at large angle, the dressing on the differential cross section for a parallel geometry covers a wide range. For a perpendicular geometry, the dressing changes the relative velocity between the incident proton and the captured electron only slightly, the laser modification in the latter case is not as significant as that in the former.

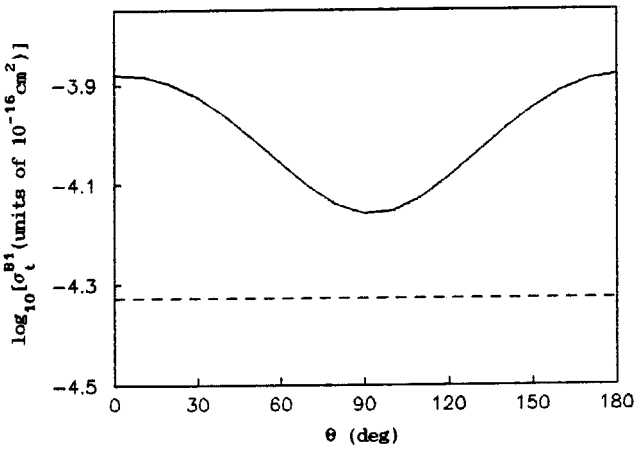

Fig. 10. Integral cross section dependence on polarization direction at $E_L = 1000$ keV, $\varepsilon_0 = 10^8\,\mathrm{V\,cm^{-1}}$, $\hbar\omega = 1.0$ eV. Solid curve: laser present. Dashed line: laser free.

The integral cross sections for both targets also exhibit distinct differences. For the dressed capture from hydrogen, the integral cross section is sensitive to the polarization direction at low energy, but for helium we find it sensitive at high energy. For hydrogen the cross section for a perpendicular geometry is higher than that for a parallel geometry; for helium, the results are contrary. The mechanism of these features comes from several different sources. Among those the difference in the electron cloud distribution between them provides an essential contribution. Because the nucleus-electron interactions contribute an important part to the electron capture cross section, and the dressing of electrons is much larger than that of nuclei, the different dressing electron states of hydrogen and helium result in the striking difference between the corresponding capture cross sections. For a helium target, the interactions among the dressed atoms and ions are much more complicated than those for an atomic hydrogen target. Fortunately, the Coulomb binding in the helium atom and in the helium ion is far stronger than that in hydrogen, and the dressing contribution to the helium atom and the helium ion is much smaller than that to hydrogen at the field strength considered. Only at the moment of collision, the laser "loosens" the helium target, which is favorable to electron capture. The dressed term of final state hydrogen plays an important role. For the capture from an atomic hydrogen target, both the dressed states of target hydrogen and the final state hydrogen have contributions to the capture cross section.

This work is supported by the Return Student Foundation of Academia Sinica, the Start Foundation for Returned Student, CRAAMD (Chinese Research for Atomic and Molecular Data), and partly supported by the National Natural Science Foundation of China. Thanks to the referee for helpful suggestions.

References

1. S.-M. Li, Y.-G. Miao, Z.-F. Zhou, J. Chen, Y.-Y. Liu, Z. Phys. D **39**, 29 (1997).
2. B.H. Bransden, M.R.C. McDowell, *Charge Exchange and the Theory of Ion-atom Collisions* (Clarendon, Oxford, 1992).
3. Dz. Belkic, R. Gayet, A. Salin, Phys. Rep. **56**, 279 (1979).
4. B.H. Bransden, *Atomic Collision Theory* (Benjamin, New York, 1970).
5. J.D. Jackson, H. Schiff, Phys. Rev. **89**, 359 (1953).
6. B.H. Bransden, A. Dalgarno, N.M. King, Proc. Phys. Soc. A **67**, 1075 (1954).
7. R.A. Mapleton, Phys. Rev. **122**, 528 (1961).
8. S.-M. Li, Z.-F. Zhou, J.-G. Zhou, Y.-Y. Liu, Phys. Rev. A **47**, 4960 (1993).
9. F.W. Byron Jr., P. Francken, C.J. Joachain, J. Phys. B **20**, 5487 (1987).
10. C.J. Joachain, *Quantum Collision Theory* (North-Holland, Amsterdam, 1983).
11. S.-M. Li, J. Chen, J.-G. Zhou, H.-J. Yin, Phys. Rev. A **47**, 1197 (1993).
12. P.J. Kramer, Phys. Rev. A **6**, 2125 (1972).
13. P.J. Martin, D.M. Blankenship, T.J. Kvale, E. Redd, J.L. Peacher, J.T. Park, Phys. Rev. A **23**, 3357 (1981).
14. P.C. Ojha, M.D. Girardeau, J.D. Gilbert, J.C. Straton, Phys. Rev. A **33**, 112 (1986).
15. C.F. Barnett, H.K. Reynolds, Phys. Rev. **109**, 355 (1958).
16. J.R. Oppenheimer, Phys. Rev. **31**, 349 (1928).
17. H.C. Brinkman, H.A. Kramers, Proc. Acad. Sci. Amsterdam **33**, 973 (1930).
18. S.-M. Li, Y. Sun, Y.-Y. Liu, Z.-F. Zhou, J. Chen, Phys. Lett. A **203**, 209 (1995).